# Trends in the Chemisorption of Aromatic Molecules on a Pt(111) Surface: Benzene, Naphthalene, and Anthracene from First Principles Calculations

**C. Morin,[†] D. Simon,[‡] and P. Sautet*,[†]**

*Laboratoire de Chimie, UMR CNRS 5182, École Normale Supérieure de Lyon, 46 Allée d'Italie, F-69364 Lyon Cedex 07, France, and Laboratoire de Spectrométrie Ionique et Moléculaire (LASIM−CNRS UMR 5579), Université Claude Bernard−Lyon I, 43 Boulevard du 11 novembre 1918, F-69622 Villeurbanne Cedex, France*

*Received: March 22, 2004; In Final Form: May 27, 2004*

The adsorption of polycyclic aromatic hydrocarbons on transition metal surfaces is of great interest to understand the possibility of their hydrogenation or their cracking in heterogeneous catalytic processes. In this paper, periodic density functional theory (DFT) calculations are presented for the comparison of the adsorption of benzene, naphthalene, and anthracene molecules on Pt(111) surfaces. For each molecule, the best adsorption structure is associated with aromatic rings on bridge sites, with increasing adsorption energies per molecule (−0.90, −1.37, and −1.79 eV, respectively), while the adsorption structures associated with aromatic rings on hollow sites are systematically less stable. Upon adsorption, molecules are distorted, which implies a modification of the energetic level and the shape of molecular orbitals, and hence ensures a better molecule−surface stabilizing interaction. The electronic analysis shows similar interactions between the molecule and the surface in each case. A model is proposed to determine the adsorption energy of larger aromatic polycyclic molecules, based on the estimation of the distortion energy of the molecule and surface, and of interaction energies between each aromatic ring and the surface.

## 1. Introduction

The chemisorption of aromatic and polycyclic aromatic molecules on a metal surface is a subject with large implications in industrial chemistry and materials science. These molecules are an undesired component of diesel and jet fuels in the petroleum industry. Their presence in the fuel decreases its performance, with a reduction of the cetane number.[1] It has also a strong environmental impact, from unburned fractions, or by favoring particulate emissions in diesel exhaust gases. The abatement of aromatic and polyaromatic fractions in diesel fuel is hence an important issue for economic and environmental reasons, and recent legislation the United States and in Europe have set a strict limit on the concentration of such molecules in fuels.[2] Catalytic processes, for example through hydrogenation or hydrogenolysis,[1,3] can be used in order to upgrade diesel fuel quality or to create more attractive molecules for fine chemistry. Both reactions take place with a transition metal catalyst, platinum being the most frequent choice. These processes are also very important for the conversion of the heavy fraction of crude oil or of coal-derived liquids where polycyclic aromatics constitute an important concentration. The adsorption of aromatic and polycyclic aromatic molecules on a platinum surface is a key elementary step in these catalytic transformations. The adsorption of polycyclic aromatic molecules is also a model for the formation of a single graphite layer on a platinum surface from hydrocarbon decomposition.[4] The formation of such a layer severely inhibits the catalytic properties,[5] and the stability of such polycyclic aromatic clusters on the surface has important implications. Such a film might have in contrast a positive aspect on the mechanical properties of the surface, acting as a lubricant.

The aim of this paper is hence to compare the chemisorption of polycyclic aromatic molecules of increasing size on a platinum (111) surface from first principles calculations, in terms of structure and energy. Condensed aromatic rings of size 1 (benzene), 2 (naphthalene), and 3 (anthracene) have been considered. To go beyond these sizes, a qualitative model has been extracted to predict the chemisorption of larger fused ring systems.

The chemisorption of the most simple aromatic molecule, benzene, on a Pt(111) surface has been studied with a large range of experimental or theoretical techniques. The reader can refer to three recent theoretical studies and references therein.[6−8] The molecule lies flat on the surface, with two competing adsorption sites, the bridge site being slightly more stable.

For the larger polycyclic aromatic molecules, the number of chemisorption studies is much more limited. Initial investigations have shown from LEED, Auger spectroscopy, and work function measurement that naphthalene adopts on Pt(111) both ordered and disordered structures. The molecule's ring is parallel to the surface, and the observed ($6 \times 3$) LEED pattern indicates that the molecule centers are separated by 3 Pt−Pt surface distances.[9−13] The key technique to address the chemisorption of such large molecule is certainly scanning tunneling microscopy (STM), since it allows us to obtain an atomic-scale image in real space of the molecule. Such images can be obtained in ultrahigh vacuum with in situ electrochemical conditions. The molecule is imaged as an elongated feature in both ordered and disordered systems, and a top binding site is tentatively suggested.[14] At low coverage, molecular rotations among favored orientations and translation between adjacent sites are observed at room temperature. The molecules are grouped in

* Corresponding author. E-mail: Sautet@ens-lyon.fr. Tel: (33) 4 72 72 81 55.
[†] École Normale Supérieure de Lyon.
[‡] Université Claude Bernard−Lyon I.

10.1021/jp048733j CCC: $27.50 
Published on Web 07/16/2004

$3 \times 3$ domains, but the molecular orientations are not fully ordered. The long naphthalene molecular axis is, however, parallel to the close-packed rows of the Pt(111) surface. High resolution images clearly show the double ring structure.[15] These results are confirmed by a more recent study in electrochemical environment.[16] The only difference is that molecular diffusion was here found to be very slow.

Anthracene was only imaged by STM on a Rh(111) surface,[16] with a fantastic resolution of the triple ring. Again the molecule long axis preferentially aligns along the close-packed direction of the surface. The adsorption of anthracene can simply be visualized by appending one more aromatic ring to the naphthalene molecule, with the center of the molecule now occupying a bridge site.

The studies of polycyclic aromatic molecule adsorption by theoretical approaches are also rare. The adsorption of naphthalene was studied from semiempirical tight-binding calculations on Pt clusters exposing a (111) surface.[17] The results suggested that naphthalene chemisorbs on a top site, with an orientation parallel to the dense metal row. Very recently, density functional theoretical calculations were used to study naphthalene adsorption on a $Pt_7$ clusters.[18] Only one structure was calculated, corresponding to the top site, and it did not significantly deviate from that calculated for benzene. It can be noted, however, that unsaturated edge atoms of the cluster are involved in the chemisorption process, due to the small size of the cluster. To our knowledge, the adsorption of naphthalene and anthracene has not been studied from first principles with a surface described by a periodic slab.

## 2. Methods

The calculation of the wave functions for the periodic system is performed with the Vienna Ab initio Simulation Package (VASP).[19,20] This code solves the Kohn−Sham equation of density functional theory (DFT), using a plane wave basis set. A good convergence was achieved with a cutoff energy of 400 eV. The projector augmented wave method,[21,22] a frozen core method which uses the exact valence wave functions instead of pseudo wave functions, has been used to describe the electron−ion interaction. The exchange and correlation effects are described through the generalized gradient approximation (GGA) by the exchange-correlation functional of Perdew and Wang (PW 91[23]). The unit cell used for periodic calculations corresponds to $p(3 \times 3)$, $p(3 \times 4)$, $p(3 \times 5)$, or $p(4 \times 4)$ superstructures for the adsorbed benzene, naphthalene, anthracene, or phenanthrene molecules, respectively. Brillouin-zone integrations have been performed using a $5 \times 5 \times 1$ Monkhorst−Pack grid[24] for benzene and naphthalene, or $5 \times 3 \times 1$ for anthracene and $3 \times 3 \times 1$ for phenanthrene, and a second-order Methfessel−Paxton smearing[25] of 0.25 eV, as these densities of *k*-points allow a good convergence of the adsorption energy.[7]

As only flat-lying molecules are observed experimentally, we have limited our adsorption structures to molecules with their aromatic rings parallel to the surface. The calculations have been performed with a metallic slab of four layers, as such a slab has been shown to be large enough to properly describe the surface.[7] During geometric optimizations, the entire molecules, as well as the uppermost two layers of the metallic surface, were allowed to relax; the two other layers of metal stayed fixed in the bulk geometry. The slab is repeated periodically in the direction perpendicular to the surface, and the vacuum space between neighboring slabs was set to an equivalent of five layers of metal, i.e., more than 13 Å in each case, which is large enough to avoid interaction between the adsorbed molecule and the periodic images of the slab. The calculations have been performed mainly on an IBM SP Power 4 computer. A typical CPU time needed for the geometry optimization is 30 days for naphthalene starting from the juxtaposition of two optimized benzene molecules.

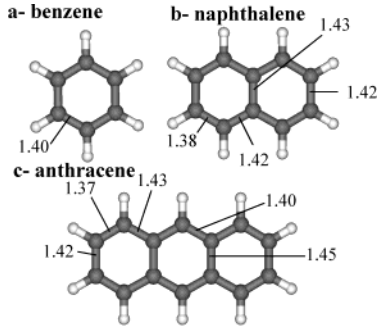


**Figure 1.** Gas-phase calculated geometry (bond lengths in angstroms) of (a) benzene, (b) naphthalene, and (c) anthracene.

## 3. Adsorption of Molecules

The optimized gas-phase geometries of benzene, naphthalene, and anthracene molecules are presented in Figure 1. The benzene molecule shows a $D_{6h}$ symmetry, with a calculated C−C bond length of 1.40 Å. The naphthalene presents two distorted aromatic cycles, with four shorter C−C bonds of 1.38 Å and six longer bonds of 1.42 Å. The C−C bond linking the two cycles is also long (1.43 Å). These values are in good agreement with experiments (around 1.37, 1.42, and 1.43 Å, respectively)[26−30] and previous calculations (around 1.37, 1.41, and 1.43 Å, respectively).[31,32] In the same way, the two exterior cycles of the anthracene molecule are distorted (two bonds of 1.37 Å and three of 1.42 and 1.43 Å), while the central cycle is less distorted (four bonds of 1.40 Å). Moreover, the bonds shared by two cycles are elongated to 1.45 Å. Once again, these values are in good agreement with experimental (1.40, 1.42, 1.44, 1.39, and 1.44 Å, respectively)[33] and calculated (with differences lower than 0.01 Å)[31] values. We can suppose that this trend will be the same for the larger molecules with four or five aligned aromatic cycles.

This section develops the adsorption and concomitant distortion of these three molecules.

**Benzene.** Experimental studies of the adsorption of benzene on Pt(111) with high-resolution electron energy loss spectroscopy (HREELS), reflection−adsorption infrared spectroscopy (RAIRS), and low-energy electron diffraction (LEED) with and without CO coadsorption[34−38] proved that the molecule is chemisorbed with its aromatic ring parallel to the surface. Moreover, these investigations, completed by theoretical studies,[7,8] showed that the interaction between the aromatic $\pi$ states and the d band of the surface is the predominant effect responsible for the adsorption of such a molecule. The periodic ordering was experimentally found to be $(2\sqrt{3}\times4)$rect$-2C_6H_6$ in the case of coadsorption with carbon monoxide,[36] which corresponds to a 1/8th coverage, and $(\sqrt{21}\times\sqrt{21})R10.9°-3C_6H_6$ in HF solution[39] (1/7th coverage). To avoid lateral interactions between molecules, we have chosen a larger unit cell $(3\times3)-1C_6H_6$ (1/9th coverage).

As previously shown in refs 7, 8, and 40, the benzene molecule can adsorb in two different structures on Pt(111) (see Figure 2): either in a bridge position (bri30) or in a 3-fold position, hcp0 or fcc0 depending on the presence of a second layer metal atom just under the molecule cycle. In contrast with

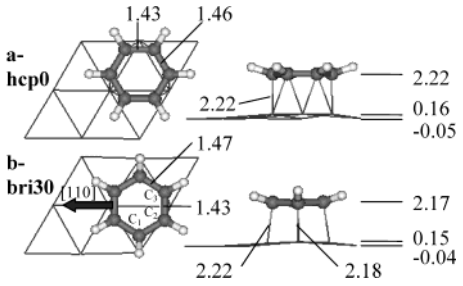


**Figure 2.** Adsorption geometry of benzene in (a) hcp0 and (b) bri30 configurations. C−C and C−Pt bond lengths are reported in angstroms. The *z* coordinates of the highest and lowest Pt atoms in the surface layer and the average *z* coordinate of C atoms in the molecule are reported in angstroms. The arrow displays the [110] direction.

the conclusions of LEED, the bri30 conformation seems to be the most stable conformation, with an adsorption energy of −0.90 eV compared to −0.67 and −0.61 eV for the hcp0 and fcc0 conformations, respectively. This conclusion is in agreement with HREELS studies, as the simulated spectra for the bri30 adsorption structure fits well the experimental spectra.[7]

In the bri30 adsorption case, the molecule presents a $C_{2v}$ distortion, due to the bridge site. The benzene molecule is bonded to four metal atoms of the surface through six carbon−platinum bonds. In the hcp0 case, the molecule adopts a Kekulé form, with three short carbon−carbon bonds (1.43 Å) above the metal atoms, and three longer bonds (1.46 Å) between metal atoms. In this case, the molecule is bonded to three metal atoms through six carbon−platinum bonds.

**Naphthalene.** No well-defined periodic structure is described by experimental studies of the adsorption of naphthalene on Pt(111). While early low-energy electron diffraction studies have proposed a periodic ordering of $(3\times3)-1C_{10}H_8$ (coverage of 1/9th) at room temperature and $(6\times6)-4C_{10}H_8$ (coverage of 1/9th) for temperatures higher than 170 °C for naphthalene on Pt(111),[9,13] two more recent scanning tunneling microscopy studies[15,16] find a disordered structure. Nevertheless, on Rh(111), naphthalene presents $(3\sqrt{3}\times3\sqrt{3})R30°-3C_{10}H_8$ at room temperature or $(3\times3)-1C_{10}H_8$ above 50 °C,[16,41] and $(4\times4)-1C_{10}H_8$ on Cu(111).[42] Hence, and as in the case of the adsorption of benzene, to avoid the lateral interaction between molecules, we have chosen a 4 × 3 unit cell in the calculations.

Figure 3 shows the different stable adsorption possibilities obtained from our DFT calculations. Some other adsorption configurations have been tried, but in each case either the relaxation process leads to one of the adsorption configurations of Figure 3 or the relaxed structure is unstable compared to the gas-phase molecule and the bare slab.

The N1 configuration corresponds to naphthalene with one aromatic ring in a hcp0 situation and the other in a fcc0 situation. Nevertheless, the molecule remains symmetric as if the presence of the second layer metal atom does not influence the adsorption geometry. Hence this configuration can be considered as a di-hollow0 structure. The N2 and N4 possibilities present di-bri30 naphthalene adsorption structures, while N3 is a di-hcp30 structure. The N5 structure differs by the fact that the naphthalene molecule is bonded to the surface by only four C−Pt bonds. The molecule is then bent with an angle of 151°, with a $C_4H_4$ species linked to the surface and a $C_6H_4$ benzene-like ring detached from the surface.

Once again, the di-bridge adsorption is favored: the adsorption energy for N2 and N4 configurations are −1.37 and −0.96 eV, respectively. The di-hollow N1 and N3 configurations are less stable with adsorption energies of −0.53 and −0.29 eV,

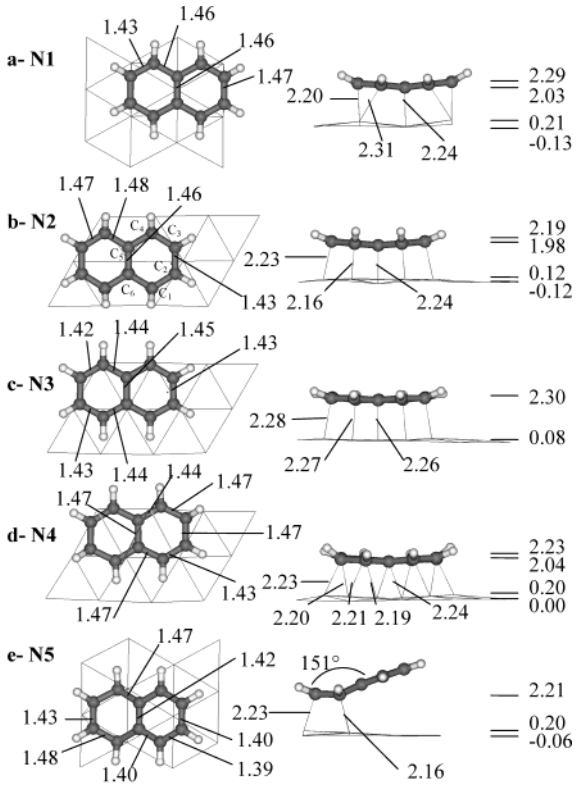


**Figure 3.** Adsorption geometry of naphthalene in (a) N1, (b) N2, (c) N3, (d) N4, and (e) N5 configurations. C−C and C−Pt bond lengths are reported in angstroms. The *z* coordinates of the highest and lowest Pt atoms in the surface layer and C atoms in the molecule are reported in angstroms.

respectively. The last N5 conformation presents an adsorption energy of −0.76 eV, relatively high compared to the adsorption energy of benzene, keeping in mind that N5 is linked to the surface through four Pt−C bonds only. This last value is however smaller than the adsorption energy of buta-1,3-diene, which has been calculated to be −1.29 [40] and −1.55 eV [43] in similar periodic calculations with 1/6th and 1/9th coverages, respectively. This can be understood because buta-1,3-diene is almost not distorted while naphthalene is strongly bent.

The N2 di-bridge adsorption configuration is the most stable structure. We can analyze its adsorption geometry and compare it with that of benzene in bri30 configuration. First, the C−Pt distances are similar in both cases (2.18 and 2.22 Å for benzene, 2.16, 2.23, and 2.24 Å for naphthalene). Second, the two cycles of naphthalene are not exactly in a bridge position but are shifted toward the $C_2$ axis, as the central C−C bond is exactly above the platinum atom of the first layer. Third, the deformation of the molecule is in the same range in both cases. For benzene, the two $C_2-C_3$ bonds (see Figure 2 for numbering) are elongated to 1.43 Å and the four $C_1-C_2$ bonds are elongated to 1.47 Å. For the naphthalene, the external $C_1-C_2$ and $C_2-C_3$ bonds are elongated to 1.43 and 1.47 Å, as for the benzene, while the internal $C_4-C_5$ and $C_5-C_6$ bonds are elongated up to 1.48 and 1.46 Å, respectively.

**Anthracene.** No ordered structure of anthracene has been experimentally observed, either on Pt(111) or on Rh(111).[16] Nevertheless, a $(4\times4)-1C_{14}H_{12}$ adlayer has been observed by STM on Cu(111),[42] and by spectroscopic techniques based on photoabsorption and photoemission on Ag(111).[44] Once again, we have chosen a 5 × 3 unit cell, to avoid lateral interactions between molecules.

**TABLE 1: Geometric and Energetic Details of Adsorption of Benzene, Naphthalene, and Anthracene**

| | bri30[a] | hcp0[a] | N1[b] | N2[b] | N3[b] | N4[b] | N5[b] | ant[c] |
|---|---|---|---|---|---|---|---|---|
| $\alpha$(CH/CCC)[d] (deg) | 23 | 19 | 19 | 26 | 14 | 21 | 15 | 29 |
| $d$(C−C) (Å) | 1.46 | 1.46 | 1.45 | 1.47 | 1.43 | 1.48 | 1.43 | 1.47 |
| $N$(metal) | 4 | 3 | 5 | 7 | 5 | 6 | 3 | 10 |
| $N$(C−Pt) | 6 | 6 | 10 | 10 | 5 | 10 | 6 | 14 |
| $d$(C−Pt) (Å) | 2.21 | 2.22 | 2.25 | 2.20 | 2.27 | 2.21 | 2.20 | 2.20 |
| $E_{ads}$ (eV) | −0.90 | −0.67 | −0.53 | −1.37 | −0.29 | −0.96 | −0.76 | −1.79 |
| $E_{dist}$(molec) (eV) | 1.51 | 0.87 | 1.32 | 2.89 | 0.70 | 1.93 | 1.66 | 4.44 |
| $E_{dist}$(surf.) (eV) | 0.33 | 0.35 | 0.64 | 0.44 | 0.28 | 0.61 | 0.29 | 0.90 |
| $E_{interaction}$ (eV) | −2.74 | −1.90 | −2.50 | −4.70 | −1.27 | −3.50 | −2.72 | −7.13 |
| $E_{interaction}/N$(metal) (eV) | −0.69 | −0.63 | −0.50 | −0.67 | −0.25 | −0.58 | −0.91 | −0.71 |

[a] Benzene adsorption configuration as presented in Figure 2. [b] Naphthalene adsorption configuration as presented in Figure 3. [c] Anthracene adsorption configuration as presented in Figure 4. [d] $\alpha$(CH/CCC), average out-of-plane angle; $d$(C−C), average carbon−carbon bond length; $N$(metal), number of metal atoms involved in molecule−surface interaction; $N$(C−Pt), number of carbon−platinum short bonds; $d$(C−Pt), average length of the N(C−Pt) short carbon−platinum bonds.

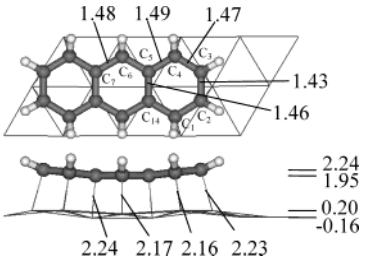


**Figure 4.** Adsorption geometry of anthracene in triple bridge configuration. C−C and C−Pt bond lengths are reported in angstroms. The *z* coordinates of the highest and lowest Pt atoms in the surface layer and C atoms in the molecule are reported in angstroms.

In this case, due to the size of the molecule and hence the size of the unit cell, only one adsorption configuration has been optimized, derived from an extension of N2 structure for naphthalene. As previously seen, the best benzene adsorption configuration is bri30, and that of the naphthalene is di-bri30. Moreover, experimental STM studies have concluded to a tri-bridge structure on Cu(111) and Rh(111).[16,42] We choose hence to optimize the tri-bri30 configuration. The geometric data of the optimized structure are presented in Figure 4. We can notice a slight boat shape, with alternatively short and long carbon−platinum bonds, similar to those optimized for benzene in bri30 or naphthalene in N2 configurations. Its adsorption energy is 1.79 eV.

## 4. Energy Decomposition

The adsorption energy can be decomposed in three different terms, each of them reflecting a characteristic of the adsorption. (i) The molecule is distorted through adsorption, and we can hence define the distortion energy of the molecule as the difference between the energy of the isolated molecule in its gas-phase geometry and the energy of the isolated molecule distorted as in the adsorption case. (ii) In a similar way, the surface is distorted while adsorption occurs, and we can define the distortion energy of the surface as the difference between the energy of the isolated bare surface and the energy of the bare surface in the distorted geometry. These two distortion energies are obviously counted positively (i.e., destabilizing). (iii) Finally, the distorted molecule and surface will interact while they meet; we define the negative interaction energy as the adsorption energy minus the sum of the distortion energies.

The different values for such an energy decomposition are presented in Table 1. The distortion energy of the molecule is directly linked to its distorted geometry. This distortion can be evaluated through the average C−C bond length and the average out-of-plane CH/CCC angle (angle between the $C_iH$ bond and its projection onto the $C_{i-1}C_iC_{i+1}$ plane). For benzene, the average C−C bond length is similar for both chemisorption structures (+4% compared to the gas phase), but the average hydrogen-tilt angle is 23° for the bri30 adsorption structure and 19° for the hcp0 structure. As a consequence, the bri30 structure has a distortion energy of 1.51 eV, much larger than that of hcp0, 0.87 eV. For the naphthalene structures, a similar trend can be observed. The N3, N1, N4, and N2 structures present elongated C−C bonds, with average values of 1.43, 1.45, 1.48, and 1.47 Å respectively, associated with increasing values for the out-of-plane CH−CCC angles of 14°, 19°, 21°, and 26°, respectively. Those values are directly linked to an increasing distortion energy of the molecule, 0.70, 1.32, 1.93, and 2.89 eV, respectively. The N5 structure is slightly different, as the molecule is in this case bent and presents two different parts. This bending of 151° strongly damages the aromaticity of the molecule, and explains the high distortion energy (1.66 eV) despite the weak C−C bond elongation (1.43 Å) and a low average out-of-plane angle of the hydrogen atoms (15°). In the case of anthracene, the high distortion energy of 4.44 eV is explained by the strong elongation of C−C bonds (1.47 Å in average) compared to the gas-phase value of 1.41 Å, the high out-of-plane angle of 29°, and a slight boat shape, as can be seen in Figure 4. Moreover, for the benzene−bri30, naphthalene−N2, and anthracene−tri-bridge series, we can correlate the distortion energies to the number of C−C bonds. In each case, the ratio $E_{dist(molec)}/N_{(C-C)}$ is almost the same (∼0.26 eV). This shows a first trend that we could use to predict the behavior of larger molecules, with four or five aromatic rings.

The distortion energy of the surface, which could be considered as low in the case of the adsorption of benzene (0.34 eV on average), must be taken into account while the molecule becomes bigger. For the naphthalene adsorption it can be as high as 0.64 eV and for anthracene, 0.90 eV. This trend can be simply explained by the number of Pt atoms involved and displaced on the surface. While benzene covers only three or four metal atoms, naphthalene covers up to seven metal atoms (in the N2 case) and anthracene 10 of them. This size increase implies that the system, in order to optimize the interaction between molecule and surface, is forced to move more and more metal atoms. This movement implies a higher distortion energy of the surface. Moreover, if we divide the distortion energy of the surface by the number of metallic atoms implied in the interaction with the molecule, we obtain a comparable average value for each molecule of ∼0.08 eV/surface atom.

We have previously shown that the adsorption energy is a compromise between the distortion of both molecule and surface and the interaction between them.[7,45] We can draw the same conclusions here for the adsorption of the polycyclic aromatic

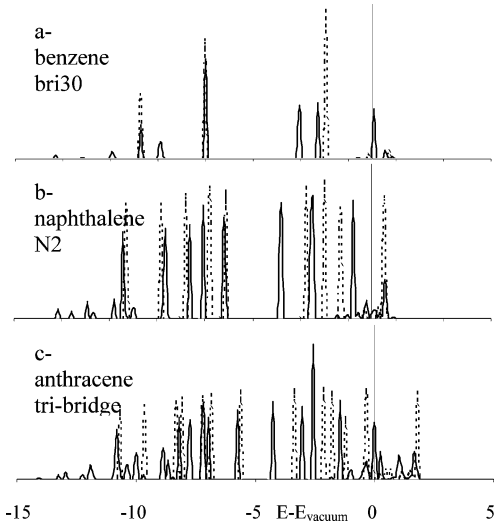


**Figure 5.** Projected density of states (PDOS) on $2p_z$(C) of (a) gas-phase benzene molecule in relaxed geometry (dashed lines) and in bri30-like distorted geometry (full line), (b) gas-phase naphthalene molecule in relaxed geometry (dashed lines) and in N2-like distorted geometry (full line), and (c) gas-phase anthracene molecule in relaxed geometry (dashed lines) and in tri-bridge-like distorted geometry (full line).

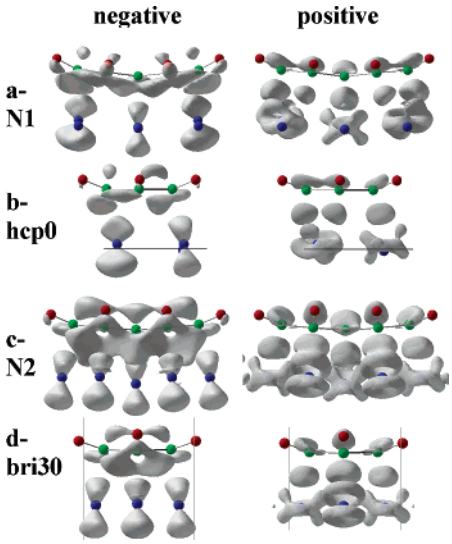


**Figure 6.** Negative (left) and positive (right) isosurfaces of the differential electron density of naphthalene in (a) N1 and (c) N2 adsorption configuration, and benzene in (b) hcp0 and (d) bri30 adsorption configuration, with respect to the distorted geometries.

molecule. A large distortion of the molecule for the N2 structure ($E_{dist}$ = 2.89 eV) is related to a large interaction energy ($E_{inter}$ = −4.70 eV), while a low distortion energy, for example for N3 structure ($E_{dist}$ = 0.70 eV), is related to a lower interaction energy ($E_{inter}$ = −1.27 eV). The two other N1 and N4 structures present intermediate values. In the cases studied here, since only one metal surface is considered, distortion energy and interaction energy also directly correlate with the adsorption energy and the most distorted structures are those with the most important adsorption energy. The anthracene tri-bridge structure, which also presents a high distortion, shows a high interaction energy ($E_{inter}$ = −7.13 eV) and a high adsorption energy ($E_{ads}$ = −1.79 eV). For each aromatic molecule case, the interaction energy of the more stable structure (bri30, di-bri30, and tri-bridge) can be easily correlated to the number of platinum atoms involved in the interaction. Table 1 reports the interaction energies divided by this number of platinum atoms. The value is very similar (−0.70 eV) for the benzene bri30, naphthalene N2, and anthracene tri-bridge structures, underlying again the scaling behavior of the system with size. However, we must keep in mind that the average length of C−Pt bonds is also important. That is why in the case of the benzene hcp0 and naphthalene N1 adsorption structures, the values of $E_{inter}/N$(metal) (−0.63 and −0.50 eV/atom) are related to the average length (2.22 and 2.25 Å, respectively).

## 5. Electronic Analysis

Figure 5 presents the projected densities of states (PDOS) on $2p_z$ orbitals of carbons of isolated benzene, naphthalene, and anthracene in gas-phase geometry (dashed lines) and respectively in bri30, N2 (di-bri30), and tri-bridge adsorption geometries (full lines). In the gas-phase geometries, the molecules are completely planar, and the $2p_z$ orbitals of carbon atoms just form the $\pi$ and $\pi^*$ orbitals. In the adsorbed geometries, because of the symmetry lowering, the $2p_z$ orbitals of carbon atoms are still the main components of $\pi$ and $\pi^*$ orbitals, but they also get small contributions in the $\sigma$ and $\sigma^*$ orbitals, and that is the reason small peaks appear near the classical peaks.

For each molecule, the differences between the two spectra reveal the electronic changes induced by the molecular distortion. The energetic gap between the highest occupied molecular orbital (HOMO) and the lowest unoccupied molecular orbital (LUMO) can be easily related to the distortion energy of the molecule. We have already shown that the gap variation is related to the molecule distortion[7] in the case of benzene. The gaps for benzene, naphthalene, and anthracene in the gas-phase geometries are 5.06, 3.38, and 2.25 eV, respectively, while for isolated distorted molecules, they are 3.94, 2.36, and 1.46 eV, respectively. The gap is hence less reduced for benzene (−1.13 eV, −22%) than for naphthalene (−1.01 eV, −30%) and for anthracene (−0.79 eV, −35%). This is correlated with the distortion energies (1.51, 2.89, and 4.44 eV, respectively.). Hence, the molecular distortion implies a stabilization of vacant molecular orbitals and a destabilization of occupied orbitals. At the same time, the carbon atoms become hybridized, to ensure a better overlap with platinum atom orbitals. Hence a high distortion implies a better electronic interaction between occupied (respectively vacant) adsorbate orbitals and vacant (respectively occupied) orbitals on the surface, from a reduced energy difference and a better orbital overlap. Finally, from benzene to naphthalene and anthracene, the HOMO−LUMO gap decreases, because both electronic delocalization and molecular distortion increase. Hence, electronic interaction between those orbitals and the metallic d band increases, which is shown by an increased interaction energy (−2.74 for benzene bri30, −4.70 for naphthalene N2, and −7.13 for anthracene tri-bridge structures).

An analysis of the electron densities has been performed for the two most stable adsorption configurations of benzene and naphthalene on Pt(111). The differential electron densities are obtained by subtracting the electron distribution of the clean surface and of the isolated molecule, both distorted as in the adsorption complex, from the charge distribution of the adsorbate−substrate complex. These densities reflect the interaction between the surface and the molecules, and not the electronic changes due to the distortion of molecule or surface. Figure 6 shows the positive and negative isosurfaces of the differential electron density of naphthalene and benzene in N1 and N2 (respectively hcp0 and bri30) adsorption configurations. The positive zones correspond to an increased electron density through adsorption, while the negative parts are electronic depletion zones.

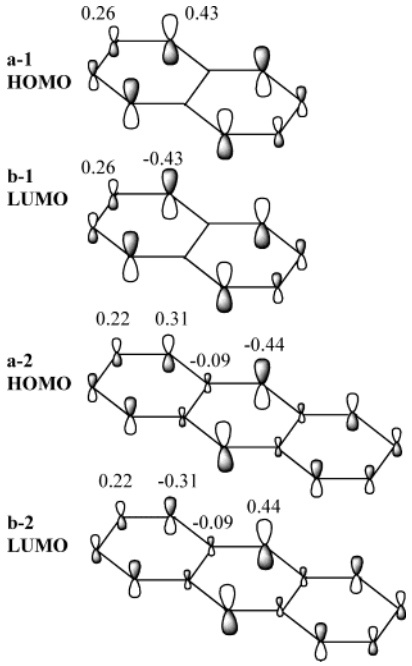


**Figure 7.** (a) Highest occupied (HOMO) and (b) lowest unoccupied (LUMO) molecular orbitals of gas-phase (1) naphthalene and (2) anthracene molecules obtained by a Hückel calculation. Numbers display the coefficients of the atomic $2p_z$ orbitals.

The electronic interactions between an aromatic molecule and a metallic surface have been described previously.[8,45] The occupied $\pi$ and vacant $\pi^*$ orbitals of the molecule interact with the mostly occupied $d_{z^2}$ and $d_{xz} + d_{yz}$ bands of the surface, to form bonding contributions at low energies and antibonding contributions at higher energies, which are generally pushed above the Fermi level, and are hence vacant. As a result, both orbitals ($\pi$ orbitals of the molecule and $d_{z^2}$ of the surface) are depopulated, which can be seen in the negative isosurfaces of Figure 6b, while the spatial zones between the carbon atoms of the molecule and the metallic atoms, and the $d_{xz} + d_{yz}$ metallic orbitals, are populated (see positive isosurfaces). Finally, we can summarize these interactions as an electronic donation from $\pi$ molecular orbitals to the $d_{xz} + d_{yz}$ band of the surface and a back-donation from the $d_{z^2}$ band to $\pi^*$ molecular orbitals.

These images can also help us to understand the similarities for the adsorption of benzene and naphthalene molecules. One can easily notice the similarities of the negative and positive isosurfaces obtained for the adsorption of naphthalene in N1 (di-hcp0) and benzene in hcp0 adsorption configurations on one hand, and naphthalene in N2 (di-bri30) and benzene in bri30 adsorption configurations on the other hand. In each case, the images for naphthalene can be seen as a 2-fold duplication of that of benzene. This proves a similar mode of adsorption of both molecules and can explain why the interaction energies are in a first approximation proportional to the number of metal atoms involved in the molecule−surface interaction.

Moreover, the population of $\pi^*$ molecular orbitals, and the depopulation of $\pi$ orbitals, explains the geometric changes of the molecule upon adsorption. Figure 7 displays the highest occupied (HOMO) $\pi$ and lowest unoccupied (LUMO) $\pi^*$ orbitals of naphthalene and anthracene isolated relaxed molecules obtained by Hückel calculations. For the naphthalene N2 adsorption structure, compared to the gas-phase geometry, the eight $C_1-C_2$ and $C_4-C_5$ bonds are elongated (+0.09 and +0.06 Å, respectively), while the other three are much less elongated (+0.03 Å for $C_5-C_6$ and +0.01 Å for $C_2-C_3$). Through adsorption and interaction with the platinum surface, the HOMO orbital is depopulated and hence the bonding character around $C_1-C_2$ and $C_3-C_4$ bonds and the antibonding character around $C_2-C_3$ bonds are lowered. At the same time, the LUMO orbital is populated, and hence the bonding character around $C_2-C_3$ bonds and the antibonding character around $C_1-C_2$ and $C_3-C_4$ bonds are increased. Finally, this simple picture explains why the $C_1-C_2$ bonds are much more elongated than the others (especially $C_2-C_3$). Similarly, for anthracene tri-bridge adsorption, the $C_2-C_3$ and $C_5-C_{14}$ bonds are almost not elongated compared to the gas-phase molecule, while the $C_3-C_4$, $C_4-C_5$, and $C_5-C_6$ bonds are strongly elongated. This can once again be explained by the specific shape of the HOMO and LUMO orbitals, and by their respective electronic depopulation and population upon adsorption.

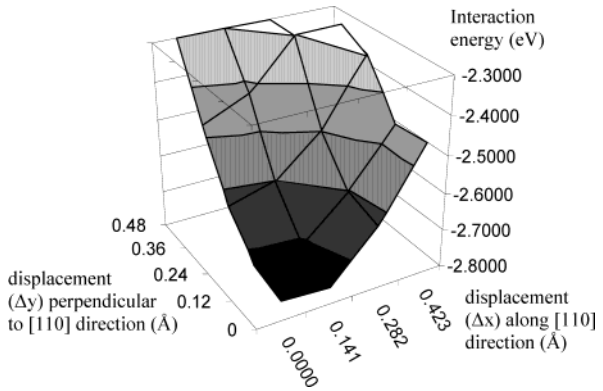


**Figure 8.** Variation of the interaction energy between benzene molecule and the platinum surface with respect to a displacement from the equilibrium bri30 site in the [110] direction ($\Delta x$) (see Figure 2) and perpendicular direction ($\Delta y$).

## 6. Trend for Adsorption Energy of Larger Molecules

We have shown that the adsorption energies result from a compromise between the distortions of surface and molecule, and the interaction between both of them. Another approach is to decompose the adsorption of a polycyclic aromatic molecule as a combination of the adsorption of each aromatic ring of the molecule. This approach can be validated by the fact that we have shown that the electronic interaction between a polycyclic molecule and the surface is similar to the interaction of several monocyclic benzene molecules with the surface. For example, the naphthalene molecule is the fusion of two different rings.

Due to the geometric constraints, these rings are not in their optimal position with respect to the surface as obtained for benzene, but they show a small lateral shift. The approach is limited to most stable situations, where each ring in the molecule is close to the bri30 site. To clarify this notion, we have performed the calculation of the adsorption and the interaction energies of benzene ring with different lateral shifts, from the most stable bri30 conformation. The results are shown in the Figure 8. The optimal molecule's position corresponds to the bri30 adsorption case ($E_{ads} = -0.90$ eV), while the other cases correspond to a lateral shift of benzene in the [110] direction ($x$ direction) and/or in the perpendicular direction ($y$ direction), as shown in Figure 8. The adsorption energy fits very well a parabola shape, with the equation

$$E^\circ_{ads}\,(\text{eV}) = -0.90 + 2.23\Delta x^2 + 1.94\Delta y^2 + 0.13\Delta x\Delta y$$

and the interaction energy between the benzene molecule and the surface fits the parabola

$$E^{\circ}_{\text{inter}}\,(\text{eV}) = -2.78 + 1.74\Delta x^2 + 2.73\Delta y^2 - 0.04\Delta x\Delta y$$

where $\Delta x$ and $\Delta y$ represent the lateral displacement of the center of the ring relative to the bri30 position, in the [110] direction and in the perpendicular direction, respectively, in angstroms. The errors between the DFT-calculated and the parabola-simulated values are less than 3.7% for the adsorption energy and 2% for the interaction energy until displacements of the benzene center of $\sqrt{\Delta x^2+\Delta y^2} = 0.42$ Å. These low errors allow us to use the parabola simulations to evaluate the DFT values in such a displacement zone.

Thanks to this last equation, we can obtain an expectation value of the interaction energy of any polycyclic molecule with the surface. Moreover, we have seen that the distortion energy of a molecule per C−C bond can be estimated to 0.26 eV, while the distortion energy of the surface is 0.08 eV per platinum atom involved in the adsorption process. Hence, to estimate the adsorption energy of a polycyclic molecule adsorbed on bri30 sites, we just need to consider it as the juxtaposition of several benzene rings and to compare its geometry to the Pt(111) surface geometry.

For naphthalene in the N2 adsorption site, each ring is moved by $\Delta x = 0.20$ Å and $\Delta y = 0$ (calculated from the relaxed isolated surface and molecule), which corresponds to $E^{\circ}_{\text{inter}}(\Delta x = 0.20, \Delta y = 0) = -2.71$ eV. This energy is the one for one $C_6$ aromatic ring interacting with four metal atoms, but as the naphthalene in the N2 structure interacts with seven metal atoms, a 7/4 coefficient must be used to evaluate its interaction energy: $E_{\text{inter}}(\text{N2,est}) = -2.71 \times 7/4 = -4.74$ eV. In parallel, the distortion energies of the molecule and the surface can be estimated to $0.26 \times 11 = 2.86$ eV and $0.08 \times 7 = 0.56$ eV, respectively. Finally, the adsorption energy, sum of these three values, is estimated to be −1.32 eV. For the anthracene molecule in the tri-bridge position, the displacement of the central ring is zero, and hence associated with an adsorption energy of $E^{\circ}_{\text{inter}}(\Delta x = 0, \Delta y = 0) = -2.78$ eV, while that of the two lateral rings is 0.40 Å, which corresponds to an interaction energy of $E^{\circ}_{\text{inter}}(\Delta x = 0.40, \Delta y = 0) = -2.50$ eV. Finally, we can estimate the interaction energy of the anthracene molecule: $E_{\text{inter}}(\text{ant,est}) = (-2.78 \times 3/4) - (2.50 \times 7/4) = -6.46$ eV (platinum atoms shared by two rings are simply associated with a weight of 0.5). As for naphthalene, we can estimate the distortion energies of the molecule and the surface to 4.16 and 0.8 eV, respectively, and, finally, the adsorption energy to −1.50 eV. For the phenanthrene molecule, adsorbed in a tri-bridge position, the same way leads to an adsorption energy of −0.96 eV (to obtain the largest simulated interaction energy, the three aromatic cycles must be displaced in $x$ and $y$ directions: one cycle is displaced $\Delta x = 0.3$, $\Delta y = 0.1$, the second $\Delta x = 0.1$, $\Delta y = 0.1$, and the third $\Delta x = 0.3$, $\Delta y = 0.24$ compared to the equilibrium bri30 position).

These three estimated adsorption energies (−1.32, −1.50, and −0.96 eV for naphthalene, anthracene, and phenanthrene, respectively), easily obtained thanks to the decomposition in terms of distortion and interaction and the superposition of interaction energies of aromatic rings, are in good agreement with the DFT-calculated energies: −1.37, −1.79, and −1.14 eV, respectively (the DFT calculation of the adsorption energy of phenanthrene has been calculated with a $k$-point mesh of $3 \times 3 \times 1$ and a unit cell of $4 \times 4$ surface atoms). The differences between the estimated and calculated adsorption energies are due to the fact that we have considered separated cycles and not juxtaposed cycles. In this last case, the molecule has generally a less important distortion energy and at the same time a less important interaction energy with the surface, to optimize the distortion−interaction compromise.

This approach is, however, a good method to obtain a qualitative and quantitative idea of the adsorption energies of larger molecules, based on the only knowledge of the molecule gas phase and of the bare surface geometries. For example, we can estimate the adsorption energy of the naphthacene (four aromatic rings in a linear chain) at $\sim -1.3$ eV and of the pentacene (five rings in a linear chain) at $\sim -0.7$ eV. When the chain length increases, the adsorption energy per molecule decreases, because the aromatic rings in the extremities of the chain are more and more shifted compared to the most stable bridge position, due to the imperfect epitaxial relation between the polycyclic aromatic molecule and the Pt(111) surface. This can be related to the misfit of a graphite adlayer on Pt(111). Indeed, a monolayer of graphite on Pt(111), which is the two-dimensional infinite analogue of the polycyclic aromatic molecules, presents a $(7 \times 7)R22$ Moiré domain,[46,47] and not a simple $(1 \times 1)$ adlayer.

## 7. Conclusion

In this paper, we have presented a quantum chemical study of the adsorption of aromatic and polycyclic aromatic molecules on Pt(111), which is an important elementary step in the catalytic transformations of such molecules. For each molecule, we have detailed the adsorption possibilities and compared them on the basis of the molecular distortion and of the electronic interactions between the molecules and the surface.

The most stable adsorption mode for the benzene molecule is the bridge mode, with the 3-fold adsorption being 0.2 eV less stable. For the polycyclic aromatic molecules, the most stable adsorption structures are also associated with rings centered on bridge sites. Situations with the rings in hollow sites are significantly less stable (0.8 eV for naphthalene, for example).

Upon adsorption, the molecules are distorted, with an increase of the ring size. This deformation can be quantified by the corresponding distortion energy. This energy itself is correlated with the interaction energy between the molecule and the surface. This is explained by the fact that the molecule distortion modifies the energetic level and the shape of the important molecular orbitals close to the surface Fermi level. The driving force for the distortion is hence to allow a better molecule−surface interaction.

The adsorption energy is a compromise between the destabilizing distortion and the stabilizing interaction. On Pt(111), this competition is dominated by the electronic interaction and hence the most stable situation is obtained for a strong interaction (and also a strong distortion).

An analysis based on the electronic structure shows that the nature of the chemical bond between the polycyclic aromatic molecules and the surface is similar to that for benzene, with no important qualitative differences, except the spatial extension.

These energetic and electronic analyses allow us to propose a model in order to estimate the adsorption energy of larger polycyclic molecules. In the model, the adsorption energy is built from the distortion energy of the molecule (obtained from the number of C−C bonds of the molecule), the distortion energy of the surface (correlated to the number of metal atoms involved in the interaction), and the molecule−surface interaction energy (estimated as the weighted sum of the values for each aromatic ring). The optimal adsorption energy per molecule

appears for the linear chain of three ring units (anthracene), and the general trend of a decrease of the adsorption energy for large systems can be explained by the geometric misfit between a graphite-like molecule and the Pt(111) substrate.

This approach based on the benzene molecule viewed as a basic building block yields a simple relation between molecular structure and adsorption on a metal surface. It also gives important insights into the adsorption energy of polycyclic aromatic molecules.

**Acknowledgment.** This work has been supported by the French computational center IDRIS (CNRS) under Contract No. 30609. We thank the Groupement de Recherche No. 12690 "Ab initio Molecular Dynamics applied to Catalysis" (CNRS), and the Institut de Recherches sur la Catalyse (CNRS) for useful scientific interactions.

## References and Notes

(1) Cooper, B. H.; Donnis, B. B. *Appl. Catal. A: Gen.* **1996**, *137*, 203.
(2) Bertelsen, B. I. *Top. Catal.* **2001**, *16/17*, 15.
(3) Stanislaus, A.; Cooper, B. H. *Catal. Rev.—Sci. Eng.* **1994**, *36*, 75.
(4) Land, T. A.; Michely, T.; Behm, R. J.; Hemminger, J. C.; Comsa, G. *Surf. Sci.* **1992**, *264*, 261.
(5) Davis, S. M.; Somorjai, G. A. In *The Chemical Physics of solid surfaces and heterogeneous Catalysis*; King, D. A., Woodruff, D. P., Eds.; Elsevier: Amsterdam, 1983; Vol. 4.
(6) Sayes, M.; Reyniers, M.-F.; Marin, G. B.; Neurock, M. *J. Phys. Chem. B* **2002**, *106*, 7489.
(7) Morin, C.; Simon, D.; Sautet, P. *J. Phys. Chem. B* **2003**, *107*, 2995.
(8) Morin, C.; Simon, D.; Sautet, P. *J. Phys. Chem. B* **2004**, *108*, 5653.
(9) Gland, J. L.; Somorjai, G. A. *Surf. Sci.* **1973**, *38*, 157. Firment, L. E.; Somorjai, G. A. *Surf. Sci.* **1975**, *55*, 413.
(10) Firment, L. E.; Somorjai, G. A. *Surf. Sci.* **1975**, *55*, 413.
(11) Firment, L. E.; Somorjai, G. A. *Isr. J. Chem.* **1979**, *18*, 285.
(12) Dahlgren, D.; Hemminger, J. C. *Surf. Sci.* **1981**, *109*, L513.
(13) Dahlgren, D.; Hemminger, J. C. *Surf. Sci.* **1982**, *114*, 459.
(14) Hallmark, V. M.; Chiang, S.; Brown, J. K.; Wöll, Ch. *Phys. Rev. Lett.* **1991**, *66*, 48.
(15) Hallmark, V. M.; Chiang, S.; Meinhardt, K.-P.; Hafner, K. *Phys. Rev. Lett.* **1993**, *70*, 3740.
(16) Yau, S.-L.; Kim, Y.-G.; Itaya, K. *J. Phys. Chem. B* **1997**, *101*, 3547.
(17) Gavezzotti, A.; Ortoleva, E.; Simonetta, M. *Chem. Phys. Lett.* **1983**, *98*, 536.
(18) de Souza, P. R. N.; Aranda, D. A. G.; Carneiro, J. W. de M.; de Oliveira, C. da S. B.; Antunes, O. A. C.; Passos, F. B. *Int. J. Quantum Chem.* **2003**, *92*, 400.
(19) Kresse, G.; Hafner, J. *Phys. Rev. B* **1993**, *47*, C558.
(20) Kresse, G.; Furthmüller, J. *Comput. Mater. Sci.* **1996**, *6*, 15.
(21) Kresse, G.; Joubert, D. *Phys. Rev. B* **1999**, *59*, 1758.
(22) Blöchl, P. E. *Phys. Rev. B* **1994**, *59*, 17953.
(23) Perdew, J. P.; Chevary, J. A.; Voslo, S. H.; Jackson, K. A.; Pederson, M. R.; Singh, D. J.; Fiolhais, C. *Phys. Rev. B* **1992**, *46*, 6671.
(24) Monkhorst, H. J.; Pack, J. D. *Phys. Rev. B* **1976**, *13*, 5188.
(25) Methfessel, M. Paxton, A. *Phys. Rev. B* **1989**, *40*, 3616.
(26) Cruickshank, D. W. J.; Sparks, R. A. *Proc. R. Soc. London, A* **1960**, *A258*, 270.
(27) Ponomarev, V. I.; Filipenko, O. S.; Atovnmyan, L. O. *Kristalographiya* **1976**, *21*, 392.
(28) Brock, C. P.; Dunitz, J. D. *Acta Crystallogr., Sect. A* **1982**, *A38*, 2218.
(29) Almenningen, A.; Bastiansen, O.; Dyvik, F. *Acta Crystallogr.* **1961**, *14*, 1.
(30) Ketkar, S. N.; Fink, M. *J. Mol. Struct.* **1981**, *77*, 139.
(31) Martin, L. M. L.; El-Yazal, J.; François, J.-P. *J. Phys. Chem.* **1996**, *100*, 15358.
(32) Sellers, H.; Pulay, P.; Boggs, J. E. *J. Am. Chem. Soc.* **1985**, *107*, 6487.
(33) Ketkar, S. N.; Kelley, M.; Fink, M.; Ivey, R. C. *J. Mol. Struct.* **1981**, *77*, 127.
(34) Lehwald, S.; Ibach, H.; Demuth, J. E. *Surf. Sci.* **1978**, *78*, 577.
(35) Cemic, F.; Dippel, O.; Hasselbrink, E. *Surf. Sci.* **1995**, *342*, 101.
(36) Ogletree, D. F.; Van Hove, M. A.; Somorjai, G. A. *Surf. Sci.* **1987**, *183*, 1.
(37) Wander, A.; Held, G.; Hwang, R. Q.; Blackman, G. S.; Xu, M. L.; de Andres, P.; Van Hove, M. A.; Somorjai, G. A. *Surf. Sci.* **1991**, *249*, 21.
(38) Haq, S.; King, D. A. *J. Phys. Chem.* **1996**, *100*, 16957.
(39) Yau, S.-L.; Kim, Y.-G.; Itaya, K. *J. Am. Chem. Soc.* **1996**, *118*, 7795.
(40) Mittendorfer, F.; Thomazeau, C.; Raybaud, P.; Toulhouat, H. *J. Phys. Chem. B* **2003**, *107*, 12287.
(41) Lin, R. F.; Koestner, R. J.; Van Hove, M. A.; Somorjai, G. A. *Surf. Sci.* **1983**, *134*, 161.
(42) Wan, L.-J.; Itaya, K. *Langmuir* **1997**, *13*, 7173.
(43) Valcárcel, A.; Clotet, A.; Ricart, J. M.; Delbecq, F.; Sautet, P. *Surf. Sci.* **2004**, *549*, 121.
(44) Annoulis, P.; Frank, K. H.; Koch, E. E. *Surf. Sci.* **1991**, *241*, 325.
(45) Morin, C.; Eichler, A.; Hirschl, R.; Sautet, P.; Hafner, J. *Surf. Sci.* **2003**, *540*, 474.
(46) Enachescu, M.; Schleef, D.; Ogletree, D. F.; Salmeron, M. *Phys. Rev. B* **1999**, *60*, 16913.
(47) Sasaki, M.; Yamada, Y.; Ogiwara, Y.; Yagyu, S.; Yamamoto, S. *Phys. Rev. B* **2000**, *61*, 15653.